Acta Crystallographica Section F
Structural Biology and Crystallization Communications
ISSN 1744-3091

Expression, purification, crystallization and preliminary crystallographic analysis of MxiH, a subunit of the *Shigella flexneri* type III secretion system needle

Janet E. Deane,[a]‡ Frank S. Cordes,[a]‡ Pietro Roversi,[a] Steven Johnson,[a,b] Roma Kenjale,[c] William D. Picking,[c] Wendy L. Picking,[c] Susan M. Lea[a,b]* and Ariel Blocker[b]

[a]Laboratory of Molecular Biophysics, Department of Biochemistry, University of Oxford, England, [b]Sir William Dunn School of Pathology, University of Oxford, England, and [c]Department of Molecular Biosciences, University of Kansas, USA

‡ These authors contributed equally to this work.

Correspondence e-mail: susan.lea@biop.ox.ac.uk

Received 21 December 2005
Accepted 21 February 2006

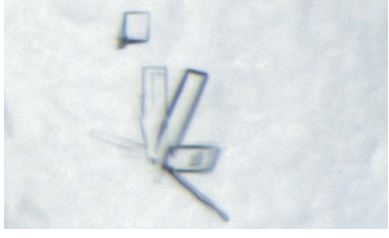

A monodisperse truncation mutant of MxiH, the subunit of the needle from the *Shigella flexneri* type III secretion system (TTSS), has been overexpressed and purified. Crystals were grown of native and selenomethionine-labelled $MxiH_{C\Delta5}$ and diffraction data were collected to 1.9 Å resolution. The crystals belong to space group *C*2, with unit-cell parameters $a = 183.4$, $b = 28.1$, $c = 27.8$ Å, $\beta = 96.5°$. An anomalous difference Patterson map calculated with the data from the SeMet-labelled crystals revealed a single peak on the Harker section $v = 0$. Inspection of a uranyl derivative also revealed one peak in the isomorphous difference Patterson map on the Harker section $v = 0$. Analysis of the self-rotation function indicates the presence of a twofold non-crystallographic symmetry axis approximately along *a*. The calculated Matthews coefficient is 1.9 Å^3 Da^{-1} for two molecules per asymmetric unit, corresponding to a solvent content of 33%.

1. Introduction

Type III secretion systems (TTSSs) are essential virulence determinants in many Gram-negative bacterial pathogens. The TTSS is required to translocate virulence effectors into the host cell. The TTSS consists of a 'needle complex' composed of an external hollow needle held within a basal body that traverses both bacterial membranes. Secretion is activated by contact of the tip of the needle complex with host cells, resulting in the formation of a pore in the host-cell membrane that is contiguous with the needle. Other effector proteins are injected *via* this apparatus directly into the host-cell cytoplasm (for a review, see Johnson *et al.*, 2005).

Many of the 25 *Shigella* proteins from which the TTSS is constructed are similar either in sequence or function to cytoplasmic and inner membrane (IM) proteins of bacterial flagellar hook-basal bodies (Blocker *et al.*, 2003). The flagellum is a helical superstructure that is assembled by the export of the flagellar components (flagellin and FlgE) through a central channel of the flagellum in a process highly analogous to the initial steps of export through a virulence TTSS (Mimori *et al.*, 1995; Yonekura *et al.*, 2003). The *Shigella flexneri* needle is composed of the ~9 kDa protein MxiH that assembles in a helical superstructure architecturally similar to the flagellar hook and filament (Cordes *et al.*, 2003; Samatey, Matsunami, Imada, Nagashima, Shaikh *et al.*, 2004; Yonekura *et al.*, 2003). A model of the innermost (D0) domain of flagellin built in a high-resolution EM map forms a tube ~70 Å in diameter with a central channel of ~20 Å, similar to the dimensions described for the *S. flexneri* needle (Yonekura *et al.*, 2003; Cordes *et al.*, 2003). Despite their different sizes and lack of sequence homology, these proteins may be structurally similar in the regions used to pack into superhelices. MxiH may thus represent the minimum core required to build a helical assembly suitable for host-cell sensing and protein export.

In *Shigella*, full-length MxiH is expressed and, following export, polymerizes to form TTSS needles (Cordes *et al.*, 2003). The needles themselves are too large and too heterogeneous in length to be amenable to crystallization. Attempts to obtain monomeric MxiH protein directly by depolymerization of the filaments and partial proteolysis were not successful. The segments of the flagellar hook and filament proteins that pack into the innermost region of the

Table 1
Data-collection statistics.

Values for the highest resolution shell are given in parentheses.

	Native	Uranyl $[UO_2(AcO_2)_2]$ soak	SeMet MAD		
			Peak (λ_1)	Remote (λ_2)	Inflection (λ_3)
X-ray source	ESRF, ID14-4	ESRF, ID14-2	ESRF, ID23		
Detector	ADSC scanner	ADSC scanner	MAR CCD		
Space group	*C*2	*C*2	*C*2		
Unit-cell parameters					
a (Å)	183.2	182.8	183.4		
b (Å)	28.1	28..0	28.1		
c (Å)	27.7	27.5	27.8		
β (°)	96.5	96.0	96.5		
Wavelength (Å)	0.976	0.9330	0.9794	0.9757	0.9797
Resolution limit (Å)	28–2.1 (2.2–2.1)	26–3.2 (3.5–3.2)	28–1.9 (2.0–1.9)	28–2.3 (2.4–2.3)	28–2.3 (2.4–2.3)
Completeness (%)	99.9 (99.9)	99.7 (99.7)	99.7 (99.4)	99.4 (99.0)	99.7 (99.1)
Unique reflections	8232	1815	11111	6408	6405
Multiplicity	4.3 (4.4)	3.1 (3.1)	4.7 (4.8)	6.7 (7.1)	6.7 (10.4)
R_{merge}†	6.6 (25.1)	14.6 (34.3)	5.4 (21.7)	10.3 (29.8)	7.8 (22.9)
$I/\sigma(I)$	7.7 (2.9)	2.4 (1.7)	5.6 (2.7)	4.0 (1.0)	5.5 (2.9)
R_{anom}‡		7.7 (15.9)	3.4 (15.4)	4.7 (10.0)	3.4 (8.5)

† $R_{merge} = 100\sum_h[\sum_i |\langle I(h)\rangle - I(h)_i|/\sum_i I(h)_i]$, where $I(h)_i$ is the ith observation of reflection h and $\langle I(h)\rangle$ is the mean intensity of all observations of h. ‡ $R_{anom} = 100\sum_h |\langle I^+\rangle - \langle I^-\rangle|/\sum_h(\langle I^+\rangle + \langle I^-\rangle)$, where $\langle I^+\rangle$ and $\langle I^-\rangle$ are the mean intensities of the Bijvoet pairs for observation h.

flagellar filament were proteolytically removed (the N-terminal 70 and C-terminal 44 residues of FlgE and the N-terminal 52 and C-terminal 44 residues of flagellin) in order to produce monomeric crystallizable forms of these subunits (Samatey *et al.*, 2000; Samatey, Matsunami, Imada, Nagashima & Namba, 2004). Here, largely owing to the small size of MxiH (9 kDa), prevention of polymerization was achieved by the removal of five C-terminal residues ($MxiH_{C\Delta5}$; Kenjale *et al.*, 2005).

2. Experimental procedures

2.1. Expression and purification

Recombinant forms of $MxiH_{C\Delta5}$ were produced and purified. The DNA fragment of the *mxiH* gene encoding residues 1–78 was produced as described previously (Kenjale *et al.*, 2005) and subcloned into the pET22b vector. This construct includes two additional residues (Leu79 and Glu80) that link the truncated form of MxiH to a C-terminal His_6 tag.

$MxiH_{C\Delta5}$ was expressed in *Escherichia coli* BL21 (DE3) cells grown in LB media containing 100 µg ml^{-1} ampicillin. Cells were grown at 310 K until an $A_{280\,nm}$ of ∼0.6 was reached, whereupon the solutions were cooled to 293 K and protein overexpression was induced by the addition of 1.0 m*M* IPTG. After ∼16 h, cells were harvested by centrifugation (15 min, 5000*g*, 277 K) and pellets were frozen at 193 K. Cell pellets were resuspended in lysis buffer (20 m*M* Tris pH 7.5, 150 m*M* NaCl and Complete EDTA-free protease inhibitor cocktail, Roche) and lysed using an Emulsiflex-C5 Homogeniser (Glen Creston, UK). The resultant cell suspension was centrifuged (20 min, 20 000*g*, 277 K) and the soluble fraction was applied to a pre-charged HiTrap HP nickel-affinity column (HiTrap Chelating HP, Amersham Biosciences). Protein was eluted using a gradient of 0–1 *M* imidazole in 20 m*M* Tris pH 7.5 and 150 m*M* NaCl. Fractions containing $MxiH_{C\Delta5}$ were further purified by gel-filtration chromatography using a HiLoad 16/60 Superdex 75 column (Amersham Biosciences). $MxiH_{C\Delta5}$ elutes in 20 m*M* Tris pH 7.5, 150 m*M* NaCl as a single slightly asymmetric peak. SDS–PAGE analysis revealed $MxiH_{C\Delta5}$ to be pure and mass-spectrometric analysis (data not shown) confirmed the molecular weight of the protein (9540 ± 1 Da). Fractions containing purified $MxiH_{C\Delta5}$ were pooled and concentrated using Centricon YM-3 centrifugal filtration devices (Millipore) to approximately 25 mg ml^{-1} and were stored at 193 K.

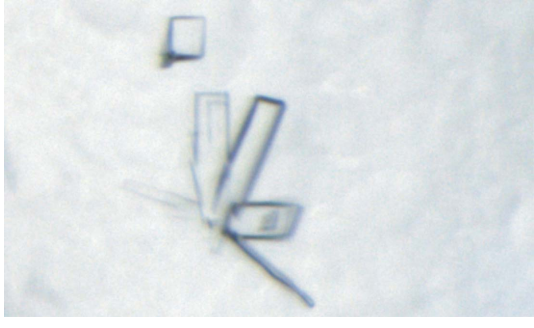

Figure 1
Monoclinic crystals of $MxiH_{C\Delta5}$. Native crystals had a longest dimension of approximately 25 µm.

The sequence of MxiH contains no methionine residues that could be exploited for preparation of selenomethionine derivatives and no cysteine residues that could be used for anomalous phasing based on sulfur. On the basis of a sequence alignment that identified a conserved hydrophobic residue at position 19 that is a methionine in the enteropathic *E. coli* (EPEC) homologue, EscF, a methionine-containing point mutant of $MxiH_{C\Delta5}$ was generated ($MxiH_{C\Delta5F19M}$). This F19M MxiH mutant in the context of wild-type *Shigella* assembled phenotypically normal needles (data not shown). SeMet-labelled $MxiH_{C\Delta5F19M}$ was produced by expression in the *E. coli met*$^-$ auxotrophic strain B834 (DE3). Cultures were grown in LB media to an $A_{600\,nm}$ of 0.9, were pelleted (15 min, 4000*g*, 277 K) and washed in PBS three times before being used to inoculate SelenoMet Medium Base containing SelenoMet Nutrient Mix (Molecular Dimensions, UK). Cells were grown and induced as described above. SeMet-labelled protein was purified as described above. Full incorporation of selenomethionine was confirmed by mass spectrometry (data not shown).

2.2. Crystallization

Initial crystallization conditions were obtained by sparse-matrix screening (Jancarik & Kim, 1991) using the sitting-drop vapour-diffusion technique. Drops were prepared by mixing 0.2 µl protein solution (25 mg ml^{-1}, 20 m*M* Tris pH 7.5, 150 m*M* NaCl) with 0.2 µl

reservoir solution and were equilibrated against 100 µl reservoir solution at 293 K. Crystals of $MxiH_{C\Delta5}$ grew overnight in condition No. 9 of Molecular Dimensions Screen 1 [20%(*w*/*v*) PEG 4000, 0.1 *M* sodium citrate pH 5.6, 20%(*v*/*v*) 2-propanol]. Crystals grown exactly as above but with the addition of 12%(*v*/*v*) glycerol to the mother liquor yielded diffraction-quality crystals of $MxiH_{C\Delta5}$ (Fig. 1). Crystals of SeMet-labelled $MxiH_{C\Delta5F19M}$ were grown as described above, except that drops were prepared by mixing 1.0 µl protein solution with 1.0 µl reservoir solution and were equilibrated against 0.5 ml reservoir solution. Diffraction-quality crystals grew in 3 days in condition No. 9 of Molecular Dimensions Screen 1 supplemented with 2%(*w*/*v*) xylitol. Uranyl derivatives were prepared by transferring $MxiH_{C\Delta5}$ crystals into a drop containing reservoir solution saturated with uranyl acetate. Crystals were soaked overnight at 293 K.

2.3. Data collection and processing

Crystals of $MxiH_{C\Delta5}$ were mounted and flash-cooled directly in the cryostream. Crystals of $MxiH_{C\Delta5F19M}$ and the uranyl derivative were cryoprotected in reservoir solution containing 15%(*v*/*v*) ethylene glycol for 15 s and flash-cooled in liquid nitrogen for data collection.

Diffraction data were recorded at 100 K (Table 1). Data were indexed and integrated in *MOSFLM* (Leslie, 1992) and scaled with *SCALA* (Evans, 1997) within the *CCP*4 program suite (Collaborative Computational Project, Number 4, 1994). Isomorphous (uranyl) and anomalous (SeMet) difference Patterson maps calculated within *autoSHARP* (Vonrhein *et al.*, 2005) using $(E^2 - 1)$ coefficients and strict outlier rejection clearly demonstrated the presence of a single site in both derivatives when calculated at a variety of resolution limits (Fig. 2). Inspection of isomorphous difference Patterson maps using the SeMet data (either between data collected at different wavelengths or compared with the native data) did not provide supporting evidence for an ordered Se within the crystals.

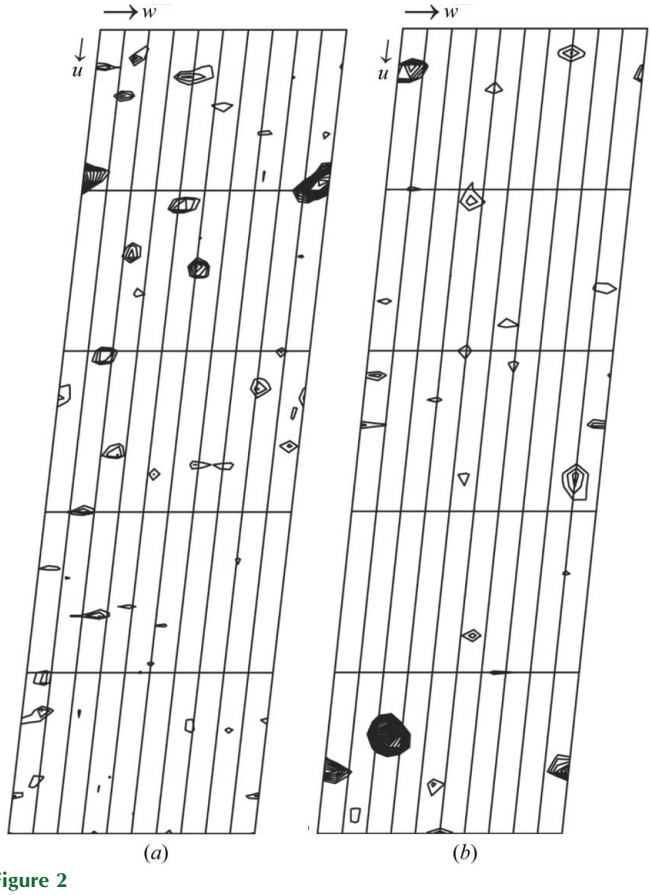

Figure 2
Difference Patterson maps of $MxiH_{C\Delta5}$. (*a*) Anomalous difference Patterson map calculated at 3.2 Å resolution with data collected at λ = 0.9794 Å (Table 1). (*b*) Isomorphous difference Patterson map for the uranyl derivative calculated at 4.3 Å resolution with data collected at λ = 0.9330 Å (Table 1). The asymmetric unit of the Harker section (*v* = 0) is shown. Maps are drawn with a minimum contour level of 1.5σ with 0.3σ increments.

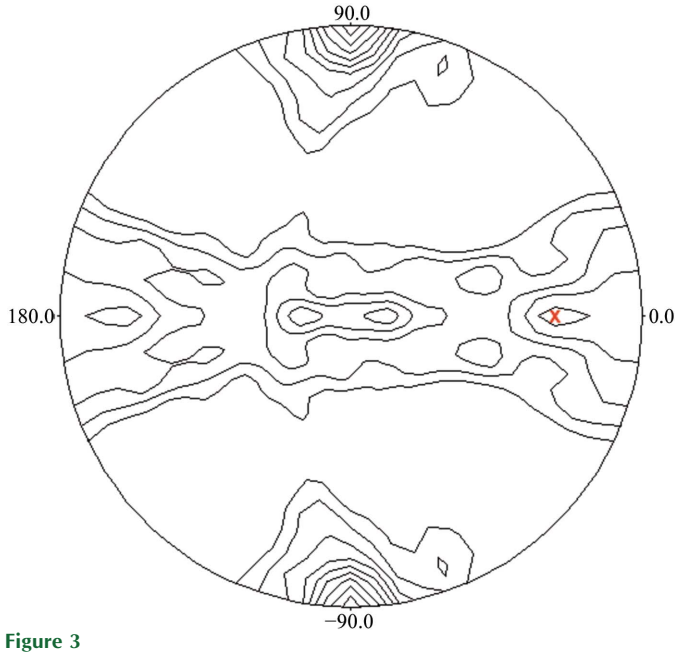

Figure 3
The κ = 180° section of the self-rotation function calculated for the SeMet peak data set using *POLARRFN* (Collaborative Computational Project, Number 4, 1994) with an integration radius of 20 Å and data in the resolution range 20–5 Å. The peak (marked with an X) at (φ, ψ) = (70.8, 0°) represents 56.5% of the peak for the crystallographic twofold.

3. Results and discussion

Rod-shaped crystals of MxiH belong to the monoclinic space group *C*2. The value of the Matthews coefficient is 1.9 $Å^3\ Da^{-1}$ for two molecules per asymmetric unit, corresponding to a solvent content of 33% (one molecule would correspond to 66% solvent content; Matthews, 1968). The self-rotation function for the SeMet peak data set (Fig. 3) indicates the presence of a twofold non-crystallographic symmetry axis almost parallel to *a* that is consistent with two molecules of $MxiH_{C\Delta5}$ per asymmetric unit but inconsistent with the observation of only a single peak in the SeMet anomalous Patterson maps. Absolute determination of the asymmetric unit contents awaits structure determination.

JED is funded by an Australian National Health and Medical Research Council CJ Martin Postdoctoral Fellowship (ID-358785) and FSC by a William R. Miller Junior Research Fellowship from St Edmund Hall, Oxford. PR is funded by a Wellcome Trust Grant (No. 077082) to SML and PR. SJ is funded by a Medical Research Council of the UK grant (G0400389) to SML and RK by a Barbara Johnson Bishop Scholarship. WDP's laboratory was supported by PHS grants AI034428 and RR017708 and the University of Kansas Research Development Fund. AB is funded by a Guy G. F. Newton Senior Research Fellowship.

References

Blocker, A., Komoriya, K. & Aizawa, S. (2003). *Proc. Natl Acad. Sci. USA*, **100**, 3027–3030.

Collaborative Computational Project, Number 4 (1994). *Acta Cryst.* D**50**, 760–763.

Cordes, F. S., Komoriya, K., Larquet, E., Yang, S., Egelman, E. H., Blocker, A. & Lea, S. M. (2003). *J. Biol. Chem.* **278**, 17103–17107.

Evans, P. R. (1997). *Jnt CCP4/ESF–EACBM Newsl. Protein Crystallogr.* **33**, 22–24.

Jancarik, J. & Kim, S.-H. (1991). *J. Appl. Cryst.* **24**, 409–411.

Johnson, S., Deane, J. E. & Lea, S. M. (2005). *Curr. Opin. Struct. Biol.* **15**, 700–707.

Kenjale, R., Wilson, J., Zenk, S. F., Saurya, S., Picking, W. L., Picking, W. D. & Blocker, A. (2005). *J. Biol. Chem.* **280**, 42929–42937.

Leslie, A. G. W. (1992). *Jnt CCP4/ESF–EACBM Newsl. Protein Crystallogr.* **26**.

Matthews, B. W. (1968). *J. Mol. Biol.* **33**, 491–497.

Mimori, Y., Yamashita, I., Murata, K., Fujiyoshi, Y., Yonekura, K., Toyoshima, C. & Namba, K. (1995). *J. Mol. Biol.* **249**, 69–87.

Samatey, F. A., Imada, K., Vonderviszt, F., Shirakihara, Y. & Namba, K. (2000). *J. Struct. Biol.* **132**, 106–111.

Samatey, F. A., Matsunami, H., Imada, K., Nagashima, S. & Namba, K. (2004). *Acta Cryst.* D**60**, 2078–2080.

Samatey, F. A., Matsunami, H., Imada, K., Nagashima, S., Shaikh, T. R., Thomas, D. R., Chen, J. Z., Derosier, D. J., Kitao, A. & Namba, K. (2004). *Nature (London)*, **431**, 1062–1068.

Vonrhein, C., Blanc, E., Roversi, P. & Bricogne, G. (2005). In *Crystallographic Methods*, edited by S. Doublié. Totowa, NJ, USA: Humana Press.

Yonekura, K., Maki-Yonekura, S. & Namba, K. (2003). *Nature (London)*, **424**, 643–650.